

LA-3921-MS

58. 1

LOS ALAMOS SCIENTIFIC LABORATORY  
of the  
University of California  
LOS ALAMOS • NEW MEXICO

VERIFIED UNCLASSIFIED  
*6/MS*  
DEC 11 1979

# Pulsed Neutron Research for Nuclear Safeguards

Program Status Report  
January-March, 1968

**FOR REFERENCE**

NOT TO BE TAKEN FROM THIS ROOM

CAT. NO. 1935

LIBRARY BUREAU

UNITED STATES  
ATOMIC ENERGY COMMISSION  
CONTRACT W-7405-ENG. 36



## NUCLEAR SAFEGUARDS RESEARCH SERIES

G. Robert Keepin, Editor

This LA...MS report presents the status of the nuclear safeguards research program at Los Alamos. Previous reports in this series are:

LA-3682-MS

LA-3802-MS

LA-3732-MS

LA-3859-MS

### LEGAL NOTICE

This report was prepared as an account of Government sponsored work. Neither the United States, nor the Commission, nor any person acting on behalf of the Commission:

A. Makes any warranty or representation, expressed or implied, with respect to the accuracy, completeness, or usefulness of the information contained in this report, or that the use of any information, apparatus, method, or process disclosed in this report may not infringe privately owned rights; or

B. Assumes any liabilities with respect to the use of, or for damages resulting from the use of any information, apparatus, method, or process disclosed in this report.

As used in the above, "person acting on behalf of the Commission" includes any employee or contractor of the Commission, or employee of such contractor, to the extent that such employee or contractor of the Commission, or employee of such contractor prepares, disseminates, or provides access to, any information pursuant to his employment or contract with the Commission, or his employment with such contractor.

LA-3921-MS  
SPECIAL DISTRIBUTION

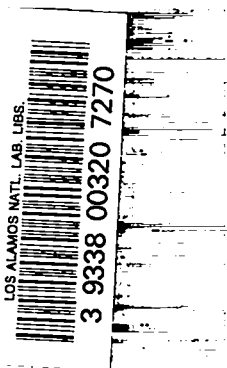
LOS ALAMOS SCIENTIFIC LABORATORY  
of the  
University of California  
LOS ALAMOS • NEW MEXICO

# Pulsed Neutron Research for Nuclear Safeguards

Program Status Report  
January-March, 1968

Distributed April 26, 1968

SCANNED JUL 21 1995



PULSED NEUTRON RESEARCH FOR NUCLEAR SAFEGUARDS

TABLE OF CONTENTS

Kinetic Response Techniques for Nondestructive Assay of Fissionable Materials	3
Absolute Delayed Neutron Yield Measurements	10
Neutron Transport Calculations	11
Auxiliary Assay Techniques Using Fission Delayed Gamma Rays	15
Detector and Instrumentation Development	18
Accelerators and Neutron Sources; Use and Development	21
Dense Plasma Focus Source	22
Other Contributions to Nuclear Safeguards Research at LASL	23

KINETIC RESPONSE TECHNIQUES FOR NONDESTRUCTIVE ASSAY  
OF FISSIONABLE MATERIALS

During the first quarter of 1968 research on kinetic response techniques progressed from experimental studies on small, rather idealized, samples to more practical, complex and heterogeneous geometries, as for example MTR fuel elements and fissionable materials in scrap barrels. The new high-efficiency slab detectors (see later section on Instrumentation and Detector Development) constitute an important addition to Group N-6's family of neutron detectors. These detectors provide a measure of the average energy of the incident neutrons and have been used to look for additional discrimination between fissionable isotopes. The large size and high efficiency of the N-6 slab detectors makes them very well suited for quantitative assay of fissionable isotopes in practical systems. This general capability has been demonstrated by recent measurements, reported herein, on fuel elements and scrap barrels. The combination of high-efficiency neutron detection and the high-intensity, versatile, neutron source provided by N-6's new "Accelerator I" (see later section on Accelerators) has reduced the time required for accurate isotopic assay and at the same time increased the sensitivity for detecting small amounts of fissionable material by substantially improving the signal to background ratio.

As has been pointed out previously, the availability of more intense neutron sources and high-efficiency neutron detectors should permit further significant increase in isotope discrimination ratios by counting for longer times after irradiation. This holds true, of course, for either instantaneous (pulsed) or saturation irradiations<sup>1</sup> (i. e.,  $R_{f+}$  or  $S_{f+/\Delta}$  measurements, as described in LA-3741).

Accordingly, the  $R_{f+}$  and  $S_{f+/\Delta}$  measurements begun last quarter have now been extended to longer counting times, and the results are summarized in Table I. All the data at  $E_n = 14$  MeV (D, T reaction) were taken using a slab detector and Accelerator I. The data at 3 MeV (D, D reaction) were taken using the N-6 Cockcroft-Walton accelerator. As expected, a significant increase in  $R_{f+}$  isotope discrimination ratio is obtained in going from the time fiducial value,  $f = 40$  sec to  $f = 150$  sec. Similarly, significant increases in  $S_{f+/\Delta}$  ratios are obtained as the time fiducial,  $f$ , is increased.

It can also be seen in Table I that, within the indicated uncertainties, the  $S_{f+/\Delta}$  ratios at (D, D) incident neutron energy agree with theoretical predictions (Los Alamos Report, LA-3741 (1967)) based on the  $a_i$ 's and  $\lambda_i$ 's from fission spectrum data. At present, direct comparisons between theory and experiment can only be made at (D, D) energy; however, when our program of measuring the  $a_i$ 's and  $\lambda_i$ 's from 14-MeV neutron induced fission is completed, direct comparison of theoretical and experimental isotope discrimination ratios will also be made at (D, T) energy.

It is of considerable practical importance to emphasize here the fact that  $^{235}\text{U}/^{238}\text{U}$  isotope discrimination ratios in excess of 2.5 are readily obtained via  $S_{f+/\Delta}$  measurements. This capability, coupled with the measurement of the independent ratios,  $R_{f-}$  (which approach a factor of 2 for  $^{238}\text{U}/^{235}\text{U}$  mixtures), provide an overall measurable isotope discrimination factor of nearly 5 between  $^{238}\text{U}$  and  $^{235}\text{U}$ . And, as noted previously, still greater effective discrimination factors are obtainable for  $^{238}\text{U}$  and  $^{239}\text{Pu}$  mixtures -- which are

destined to assume great practical importance in the coming era of fast power-breeder reactors.

TABLE I  
 $R_{f^+}$  AND  $S_{f^+/\Delta}$  ISOTOPE DISCRIMINATION RATIOS

<u><math>R_{f^+}</math> DISCRIMINATION RATIOS</u>					
$E_n \simeq 14$ MeV (D, T reaction; Irradiation Time: 0.050 sec; Total Counting Time: 300 sec)					
	<u>f = 40 sec</u>	<u>f = 100 sec</u>	<u>f = 150 sec</u>	<u>f = 200 sec</u>	<u>f = 250 sec</u>
$^{235}\text{U}/^{238}\text{U}$	1.62 ± .02	1.91 ± .04	2.18 ± .07	1.97 ± .09	1.76 ± .14
<u><math>S_{f^+/\Delta}</math> DISCRIMINATION RATIOS</u>					
$E_n \simeq 14$ MeV (D, T reaction; Irradiation Time: 150 sec; Total Counting Time: 300 sec)					
	<u>f = 50 sec</u>	<u>f = 100 sec</u>	<u>f = 200 sec</u>	<u>f = 250 sec</u>	
$^{235}\text{U}/^{238}\text{U}$	1.97 ± .1	2.28 ± .12	2.69 ± .15	2.80 ± .16	
$E_n \simeq 3$ MeV (D, D reaction; Irradiation Time: 322 sec; Total Counting Time: 300 sec)					
	<u>f = 50 sec</u>		<u>f = 100 sec</u>		
	Measured	Theory	Measured	Theory	
$^{235}\text{U}/^{238}\text{U}$	2.06 ± .07	2.18	2.56 ± .08	2.59	

### Neutron Multiplication Effects in Active Interrogation Methods

When the fission reaction ( $[n, f]$  or  $[\gamma, f]$ ) is used in the active interrogation of fissionable material, neutron multiplication effects in the sample may influence the quantitative determination of amount of fissionable material present. These multiplication effects can be important in basic fission measurements, such as absolute neutron yields, as well as in practical safeguards systems for quantitative nondestructive assay.

Measurements have been performed to determine the magnitude of neutron multiplication effects for the case of 14-MeV incident neutrons on

disc-shaped samples of  $^{235}\text{U}$  and  $^{238}\text{U}$ . For these measurements, 2"-diameter discs of  $^{235}\text{U}$  (93% enriched) and  $^{238}\text{U}$  (0.3% depleted) were placed 5" from a (D, T) neutron source, and a high-efficiency long counter was positioned 8" from the samples. The 14-MeV (D, T) neutron source was repetitively pulsed (0.10 sec irradiations followed by 0.10 sec counting intervals), and delayed neutrons from the sample were counted with the long counter. Alpha particles from the  $T(d, n)\alpha$  reaction were used to monitor the source neutron production rate.

Various sample thicknesses were used, rang-

ing from 0.010" to 0.460". Measured delayed neutron yield per gram of uranium as a function of sample thickness is shown in Figs. 1 and 2 for  $^{238}\text{U}$  and  $^{235}\text{U}$ , respectively. If there were no multiplication, absorption, or scattering of the incident and delayed neutrons, the curves in Figs. 1 and 2 would be approximately straight horizontal lines normalized to a yield of 1.0. For thicknesses less than 0.100", the observed neutron multiplication increases almost linearly with a slope of 0.268%/mil for  $^{235}\text{U}$  and 0.085%/mil for  $^{238}\text{U}$ . Thus the multiplication effect in the  $^{235}\text{U}$  is roughly a factor of 3 greater than in the  $^{238}\text{U}$  samples. It is also seen that, as sample thickness increases beyond 0.100", the rate of increase of delayed neutron yield diminishes, presumably due to competitive neutron absorption and scattering processes.

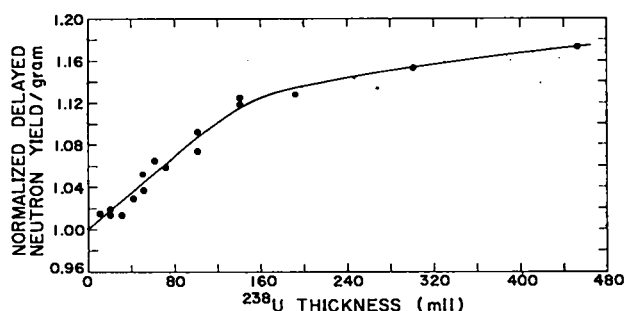


Fig. 1. Delayed neutron yield (multiplication) from 14-MeV irradiation of  $^{238}\text{U}$ .

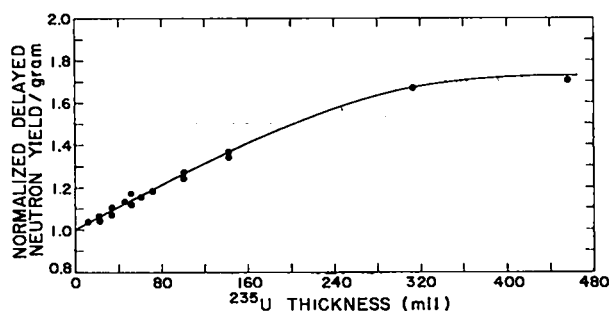


Fig. 2. Delayed neutron yield (multiplication) from 14-MeV irradiation of  $^{235}\text{U}$ .

In order to examine these various competing effects in detail, multigroup transport calculations using the DTF neutron transport code are being performed to determine the expected multiplication for disc samples, as well as spherical samples and other geometries, in a 14-MeV neutron beam. Results of these transport calculations, and comparisons with experimental data on multiplying subcritical systems, will be presented in the next quarterly program status report.

#### Energy Discrimination Between Fission Isotopes Using Slab Detectors

As noted previously, the N-6 slab detectors can provide a direct measure of the average energy of a neutron spectrum via the observed ratio of counting rates in the front and back counter banks of the slab detector. To take advantage of this energy discrimination capability, the delayed neutron kinetic response of  $^{235}\text{U}$  and  $^{238}\text{U}$  was measured in both front and back counter banks. The detector configuration was that of maximum energy discrimination (see section on Detector Development). Figure 3 shows the two response curves for  $^{235}\text{U}$ , normalized to equal counts at  $t = 0$ . It can be seen that the curves diverge at longer times, indicating that the average energy of the delayed neutron groups changes (decreases) with time. Based on the slab-detector energy calibration curve (see Detector section), some 100 keV decrease in average energy is indicated between neutrons detected at 1 sec and at 30 sec after the irradiation. When a thicker  $^{235}\text{U}$  sample was used, the average energy increased over this same time interval. This increase is due to the higher-energy prompt fission neutrons produced by sample multiplication effects, i. e., by delayed neutrons causing additional fissions in the larger sample.

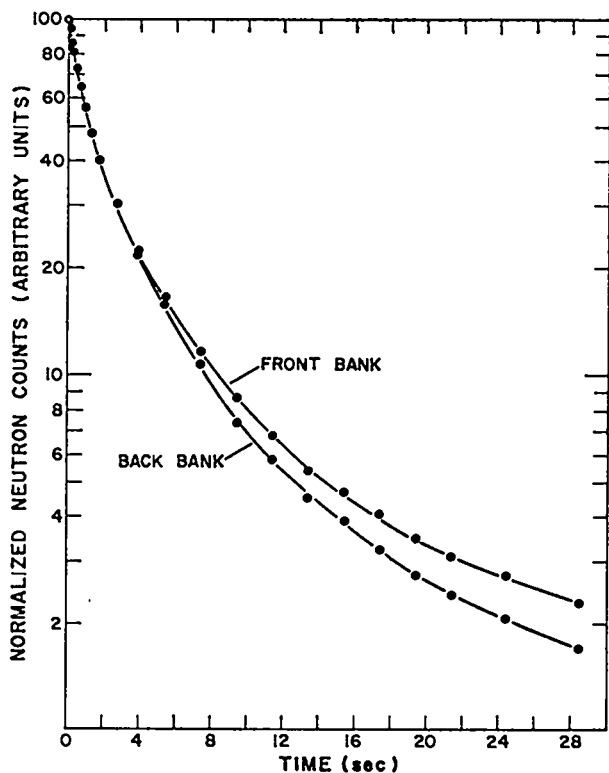


Fig. 3. Delayed neutron kinetic decay curves for  $^{235}\text{U}$  measured in front and back counter banks of the N-6 slab detector. (Normalized to equal counts at  $t = 0$ .)

The increase in isotope discrimination between  $^{235}\text{U}$  and  $^{238}\text{U}$  over that obtained with a flat-response detector (based on kinetic characteristics only) is 15%. Although this is clearly not a large increase, the ability to detect small shifts in average neutron energy can be used to advantage in some practical assay applications. For example, in the case of an unknown sample inside a closed container (e. g., the scrap barrel configuration), a shift in average neutron energy can indicate the presence of hydrogenous or moderating material.

The energy discrimination capability of slab detectors is clearly limited, but they do provide a direct measure of the average energy of a neutron spectrum, which information is itself extremely useful in many situations. Needless to say, the

slab detectors are not to be compared with true neutron spectrometers which are capable of good differential energy resolution (at some sacrifice of overall detection efficiency, of course). Based on our present knowledge of delayed neutron group spectra (cf. "Physics of Nuclear Kinetics," Addison-Wesley, p. 94 (1965)), one may anticipate significantly greater improvement in isotope discrimination factors using neutron spectrometers than the nominal 15% increase obtained with slab detectors.

#### Nondestructive Assay of Reactor Fuel Elements

In order to investigate the accuracy and practicality of delayed neutron techniques for measuring absolute amounts of fissionable material in reactor fuel elements, a series of measurements have been performed on an MTR-type fuel element mock-up. The mock-up element, shown in Fig. 4, has overall dimensions of approximately 4" x 4" x 18" and is made up of 18 parallel fuel plates. Each plate consists of a 0.001"-thick foil of  $^{235}\text{U}$  (93% enriched) sandwiched between two 0.030" sheets of Al. This gives essentially the same loading density and uranium-to-aluminum ratio as found in a typical MTR fuel element. The total amount of  $^{235}\text{U}$  in the element (with all 18 plates inserted) is 339.95 grams.

For neutron interrogation, the element was placed 12" from the (D, T) source ("Accelerator I") with the neutron beam axis perpendicular to the face of the fuel plates. The accelerator beam was modulated at approximately a 50% duty cycle (0.150 sec irradiation, 0.200 sec counting), and the delayed neutrons from the induced fission were detected with an N-6 slab detector positioned 12" behind the element. In order to vary the mass of uranium in the fuel element during the measurement, individual uranium foils were removed one at a time from the element.



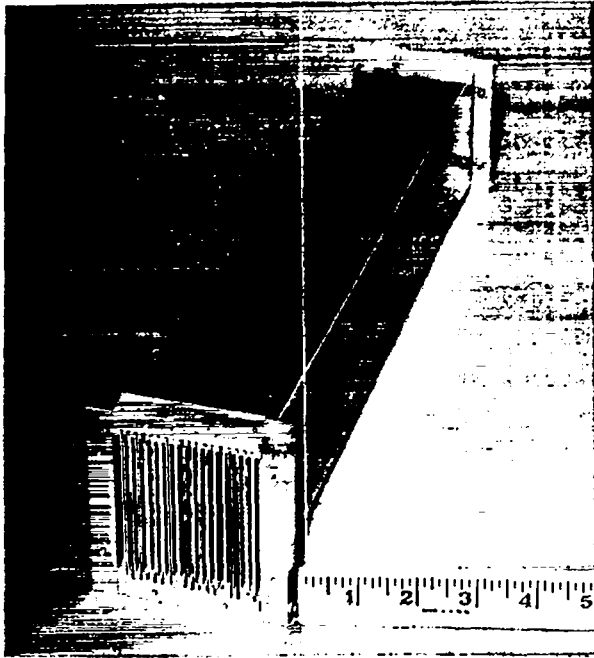


Fig. 4. Mock-up of MTR fuel element.

Because of neutron absorption and geometric effects, the effectiveness for counting a given foil ("fuel plate") of uranium will depend on its location in the fuel element. In order to minimize this unwanted position dependence, initially the distance from the element to the slab detector was adjusted so that the addition of a foil of uranium on the front side of the element gave the same increase in delayed neutron count as did the addition of a foil on the back side of the element.

The counting efficiency was calibrated using the full fuel element (18 plates) in the standard interrogation geometry, and the production rate of the neutron source was monitored with a small  $^{235}\text{U}$  fission ionization counter positioned about 6" from the (D, T) source at a back angle to the beam axis.

The results of the measurement using 14-MeV neutrons are included in Table II. It is apparent that the mass of uranium as determined from delayed neutron response agrees very closely (average deviation = 0.4%) with the actual weighed mass.

TABLE II  
DELAYED NEUTRON ASSAY OF ABSOLUTE  
AMOUNTS OF FISSILE MATERIAL  
IN MTR-TYPE FUEL ELEMENTS

<u>14-MeV (D, T) Interrogating Neutrons</u>	
<u>Actual Weighed <math>^{235}\text{U}</math> Content (grams)</u>	<u>Delayed Neutron Assay Determination (grams)</u>
339.95 (fully loaded)	Calibration Point
320.95	320.9
302.15	303.2
283.95	283.5
265.45	266.5
247.05	249.9
<u>Average Deviation: 0.4%</u>	

<u>Moderated-Spectrum Interrogating Neutrons</u>	
<u>Actual Weighed <math>^{235}\text{U}</math> Content (grams)</u>	<u>Delayed Neutron Assay Determination (grams)</u>
339.95 (fully loaded)	Calibration Point
320.95	325.3
321.15	323.3
321.75	322.6
303.25	306.0
<u>Average Deviation: 0.7%</u>	

Table II also shows the results obtained when the 14-MeV source neutrons were moderated by 4" Pb, 3" C, and 1"  $\text{CH}_2$ . The moderator was covered with a Cd foil so that only the epi-cadmium portion of the 1/E-spectrum neutrons were used for interrogation of the fuel element. Of course, the 1/E moderated neutron spectrum is somewhat more vulnerable to scattering and resonance absorption in the fuel element, and hence somewhat less penetrating than 14-MeV neutrons. Nevertheless, the mass of uranium as determined from delayed neutron measurements with either 14-MeV or 1/E-spectrum neutron interrogation is in good agreement with the actual mass, and the average deviation of 0.7% in the case of the epi-cadmium moderated spectrum is not greatly different from the deviation observed for the 14-MeV irradiation.

For reactor fuel elements in which the isotopic enrichment is unknown or in doubt, one may apply the delayed neutron kinetic response technique of isotopic analysis as reported in the previous LASL program status report (cf. LA-3859-MS). To demonstrate this technique in a practical situation, a cold, clean MTR fuel element (obtained from the OWR reactor group at LASL) was isotopically analyzed by the kinetic response method. The resulting measured isotopic abundance agreed with the actual isotopic abundance to within 1%. The comparison standards used for this assay determination were standard 2" disc samples (2" diameter, 0.010" thick) sandwiched between aluminum discs of thickness comparable to that of the aluminum cladding in a fuel element. For greater precision, the thickness of the fissile material in the comparison standard should also be comparable to that in the fuel element (18 plates, each with 0.001" equivalent  $^{235}\text{U}$  thickness). When much thicker fissile standards (0.400") were used, the indicated abundance of  $^{235}\text{U}$  in the element was low by 8%. This is due, of course, to greater multiplication in the thick  $^{235}\text{U}$  standard as compared to the thin  $^{235}\text{U}$  plates in the fuel element. (Multiplication effects in  $^{238}\text{U}$  samples are generally small compared to those in  $^{235}\text{U}$ .)

#### Fissile Material Assay in Scrap Barrels

An important practical problem in special nuclear material accountability is the determination of the amount of fissile material in common scrap containers. Delayed neutron kinetics and yield measurements offer a promising method for quantitative scrap assay. Basically, the method consists of irradiating the scrap container with a neutron source and then measuring the delayed neutrons resulting from the induced (n, f) reactions in the fissile material. Preliminary measurements have been performed to determine the sensitivity for detecting a small amount of fissile material in a standard 55-gallon steel barrel. The experimental arrangement, using the compact "Accelerator I" and two high-efficiency slab detectors, is shown in Fig. 5. The front face of each detector is covered with a sheet of cadmium 0.030" thick. A small fissile sample (10 grams of  $^{235}\text{U}$ ) was placed in the center of the 55-gallon barrel and the accelerator beam was modulated to give a repetitive series of 1-sec neutron irradiations alternating with 1-sec counting intervals. (It may be noted that this "beam modulation" technique is very similar to that used in the absolute delayed neutron yield measurements described in earlier quarterly reports.)

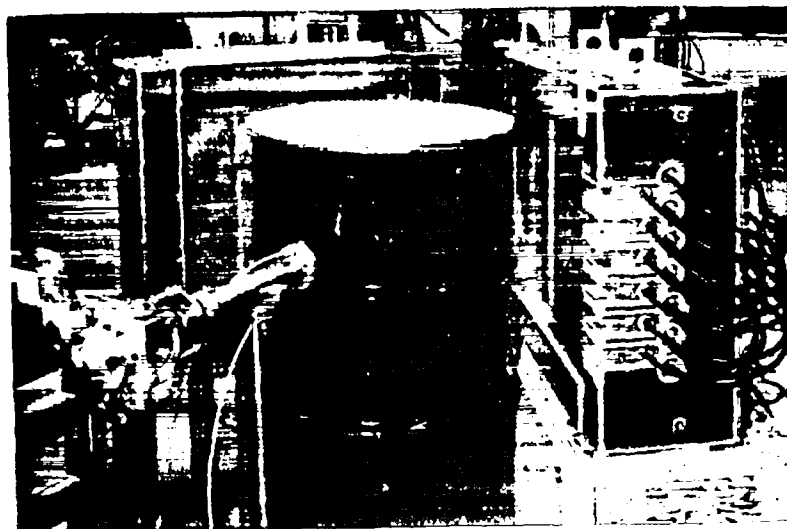


Fig. 5. Experimental arrangement for assay of fissile material in scrap barrels.

To study the effects of neutron source moderation in scrap assay, an 8" thick moderating assembly (4" Pb, 3" C, 1" CH<sub>2</sub>, covered by 0.016" Cd) was inserted between the (D, T) source and the scrap barrel. Measured delayed neutron counting rates for the various irradiation configurations are given in Table III.

The indicated delayed neutron counting rates correspond to 10 grams of <sup>235</sup>U in the center of the 55-gallon barrel; for this representative experimental arrangement (excluding, for the moment, shielding, scattering effects, etc., to be discussed later), it is clearly quite feasible and practical to detect as little as 1 gm. of fissile material in a 55-gallon barrel. To gain some very preliminary insight into the effect of hydrogenous or moderating material distributed inside the barrel, the fissile sample was surrounded by 2" of polyethylene. The result, shown in Table III, is not a decrease but a distinct enhancement of neutron counting rates as observed outside the barrel. It is clear that delayed neutron counting rates could also be increased significantly by placing a neutron reflector, such as graphite, around the outside of the barrel for 1/E-spectrum neutron irradiations. This alternative approach will be studied in some detail both experimentally and theoretically.

To observe the effect of sample position within the barrel on delayed neutron counting rate, the sample was moved radially one-half of the distance from the center to the periphery of the barrel, and the barrel was rotated through 360° during data collection. The resulting change in the counting rate for this representative asymmetric sample position was less than 6% for the 1/E-spectrum irradiations.

Use of the 1/E-spectrum for scrap interrogation has two distinct advantages over 14 MeV interrogation: (1) signal-to-background ratio increases markedly due to the larger fission cross sections of the fissile species at lower incident neutron energies, and (2) most of the neutrons are below the threshold (~ 8 MeV) for the <sup>17</sup>O(n, p) <sup>17</sup>N and other (n, 2n) and (n, p) reactions which can yield unwanted delayed neutrons and other extraneous background contributions.

It is planned in future measurements to include representative absorbing, moderating, and scattering materials interspersed with fissile material in scrap barrels. These effects are now being calculated in detail using neutron transport computer codes (see later section on transport theory calculations).

TABLE III  
MEASUREMENT OF DELAYED NEUTRONS FROM <sup>235</sup>U  
IN A 55-GALLON BARREL

<u>Delayed Neutron Counting Rate from 10 gms. of <sup>235</sup>U (cpm)</u>	<u>Total Background (cpm)</u>	<u>Energy Spectrum of Interrogating Neutrons</u>
3,000	1,290	14 MeV
4,500	725	~ 1/E Spectrum (epi-cadmium only)
16,300	725	~ 1/E Spectrum (no cadmium cover)
44,000	725	~ 1/E Spectrum (with 2" of CH <sub>2</sub> surrounding sample)

## ABSOLUTE DELAYED NEUTRON YIELD MEASUREMENTS

During the past quarter several improvements and modifications have been made to the absolute delayed neutron yield measuring techniques described in earlier progress reports. In addition, yield-vs-energy measurements have been extended to the  $^{239}\text{Pu}$  and  $^{233}\text{U}$  isotopes. The first modification was the introduction of a new long counter, "Brightman," used to measure the delayed neutrons from the sample. The counter is quite similar to the original Hansen-McKibben design, except that five  $^3\text{He}$  detectors are used instead of one  $\text{BF}_3$  detector as in the original design. The new counter has an absolute efficiency of  $1.1 \times 10^{-3}$  with the sample 17" from its front face; its efficiency is constant to within 3% as determined by Sb-Be, Pu-Li-F, and  $^{252}\text{Cf}$  sources having average neutron energies of approximately 0.025, 1.0, and 2 MeV. The second modification consisted of sandwiching the disc-shaped fission sample between two fission chambers. The number of fissions in the sample is now determined by averaging the response of the two chambers, thus taking account of any significant changes in neutron flux across the sample. The third modification

consisted of placing the fission chamber - sample assembly on the end of a long arm which could be remotely operated and swung out of the way of the neutron beam. This allowed background to be determined accurately and quickly, both before and after each run, without changing any of the accelerator controls. And fourth, the accelerating potential of the Cockcroft-Walton was increased to 325 kV in order to increase the neutron output when using the lower-yield (D, D) reaction.

Figure 6 shows the experimental arrangement used in the delayed neutron yield measurements. Just to the left of center is the detector, "Brightman," with its cadmium cover removed to show the five  $^3\text{He}$  detectors. On the right is seen the end of the accelerator beam tube and the target with its water cooling connections. Just beyond the target are the two fission chambers with the fission sample sandwiched between them. The fission chambers are attached to the remotely operated arm (seen projecting up from the bottom of the figure), which swings the entire counter - sample sandwich assembly away from the neutron source for background measurements.

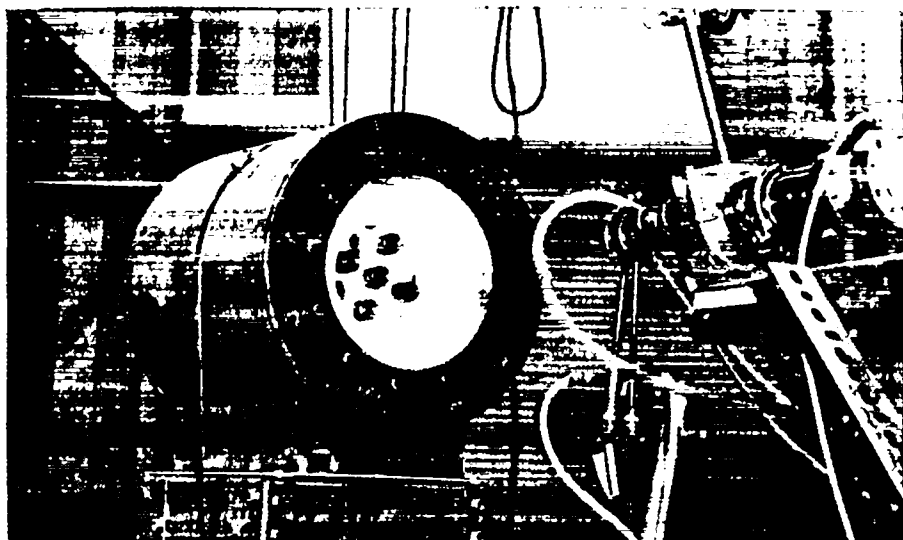


Fig. 6. Experimental arrangement for delayed neutron yield measurement.

Delayed neutron yield determinations from approximately 115 runs on five isotopes are summarized in Table IV. Pending a more complete error analysis and some auxiliary experiments necessary to confirm detector response and foil weights, a somewhat arbitrary, and quite liberal, error of  $\pm 25\%$  has been tentatively assigned to these results.

It is clear from Table IV that the previously reported decrease in absolute delayed neutron yield

in going from 3-MeV to 14.9-MeV neutron induced fission is now confirmed for each of the five major isotopes studied. This apparent general behavior of delayed neutron yield vs. incident neutron energy is consistent with theoretical expectations based on fission mass and charge distributions, but stands in striking contrast to previous measurements by other experimenters both in the U. S. A. and the U. S. S. R.

TABLE IV  
MEASURED ABSOLUTE DELAYED NEUTRON YIELDS  
(Delayed Neutrons/Fission)

	<u>3 MeV Fission</u>	<u>14.9 MeV Fission</u>	<u>Yield Ratio: <math>\frac{3 \text{ MeV}}{14.9 \text{ MeV}}</math></u>
$^{239}\text{Pu}$	.00710	.00434	1.64
$^{233}\text{U}$	.00765	.00435	1.76
$^{235}\text{U}$	.0174	.00919	1.89
$^{238}\text{U}$	.0489	.0283	1.73
$^{232}\text{Th}$	.061	.0309	1.97

### NEUTRON TRANSPORT CALCULATIONS

#### Optimum Moderator Configurations

Neutron transport calculations using the DTF-IV transport code have been directed toward maximum neutron leakage and desired spectral characteristics from various moderator assemblies. Calculations were performed in spherical geometry with a 0.5 cm diameter, distributed neutron source at the center of a moderating sphere. Both a 14 MeV source and a fission source were used. Each moderator assembly consisted of concentric spherical shells of various materials with varying radii.

It was desired to moderate the source neutrons to produce both a 1/E-spectrum and a "fast

moderated spectrum." The criterion for a "good" 1/E moderator was maximization of the fraction of leakage neutrons with energies less than the  $^{238}\text{U}$  fission threshold, and simultaneous maximization of the fraction of neutrons with energies less than 0.1 MeV. Such a spectrum would provide optimum discrimination against the threshold fissioning isotopes, e. g. ,  $^{238}\text{U}$ , while greatly enhancing the response of the fissile isotopes of major interest, notably  $^{235}\text{U}$  and  $^{239}\text{Pu}$ .

The criterion for a "good" fast moderator was a maximum number of neutrons with  $E_n < ^{238}\text{U}$

threshold energy, and a minimum number with  $E_n < 0.1$  MeV. Such a spectrum preserves neutron penetrability while still discriminating against  $^{238}\text{U}$ .

The various moderator configurations which appear to be optimum are listed in Table V. A polyethylene moderator having a 10-cm radius is included for comparison. The notation, Pb/C/CH<sub>2</sub> - 12/10/2.5, indicates a 12-cm-radius core of lead surrounded by a 10-cm-thick spherical shell of carbon surrounded by a 2.5-cm-thick shell of polyethylene. The thin shell of polyethylene surrounding all of the 1/E moderators is necessary to enhance the 1/E tail at low energies.

Two different 1/E moderators were calculated for the 14-MeV source. Moderator number 2 (cf. Table V) consists of lead, carbon, and polyethylene materials which are readily available. Moderator number 3 consists of tungsten, beryllium, and polyethylene. The tungsten non-elastic cross section near 14 MeV is about the same as that for lead, but does not fall off as rapidly in the region of a few MeV. Furthermore, the nuclear density of tungsten is approximately twice that of lead, and the nuclear density of beryllium is considerably higher than that for carbon. For these

reasons, the radius of the W/Be/CH<sub>2</sub> moderator is only 13 cm, as compared to a radius of 24.5 cm for the Pb/C/CH<sub>2</sub> combination. This impressive reduction in moderator size and weight is obtained without significantly changing the resulting neutron spectrum. In addition, the W/Be/CH<sub>2</sub> spectrum exhibits a very desirable minimum just above the  $^{238}\text{U}$  threshold (due to inelastic scattering in tungsten), while the somewhat less favorable Pb/C/CH<sub>2</sub> moderator has a maximum in this energy region. The isotopes of lead, because of their proximity to the doubly-magic nuclear mass number 208, have smaller energy level densities and, hence, lower inelastic neutron scattering cross sections than the tungsten isotopes.

The DTF-IV calculated spectra for the various moderator configurations are shown in Figures 7 and 8. An E x N(E) type of plot was chosen for the 1/E moderators in Fig. 7 since this best shows the relative numbers of neutrons in the low energy region. Figure 8 shows the leakage spectra from a tungsten "fast moderator" assembly for both 14 MeV and fission-spectrum primary sources. These results show in a very striking manner the desired spectrum peaking effect just below the  $^{238}\text{U}$  threshold.

TABLE V  
MODERATOR CONFIGURATIONS

Moderator Configuration Number	Moderator Configuration (Thickness in cm)	Neutron Source	Total Leakage	Fraction of Neutrons with $E_n < 0.1$ MeV	Fraction of Neutrons with $E_n < ^{238}\text{U}$ threshold
1	CH <sub>2</sub> - 10	14 MeV	89.9%	9.9%	16.8%
2	Pb/C/CH <sub>2</sub> - 12/10/2.5	14 MeV	141.5%	61.7%	82.5%
3	W/Be/CH <sub>2</sub> - 8/2.5/2.5	14 MeV	114.6%	61.8%	80.1%
4	W/Be/CH <sub>2</sub> - 5/5/2.5	Fiss.	77.5%	69.2%	88.7%
5	W-10	14 MeV	139.0%	15.2%	86.6%
6	W-10	Fiss.	86.4%	16.2%	88.4%

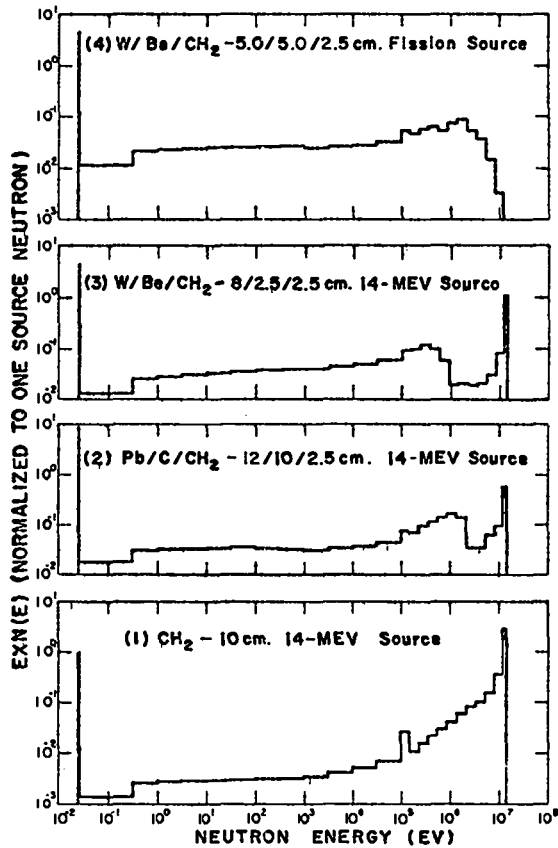


Fig. 7. Neutron leakage spectra from  $1/E$  moderator assemblies. (Note change in ordinate scales, all normalized to one source neutron.)

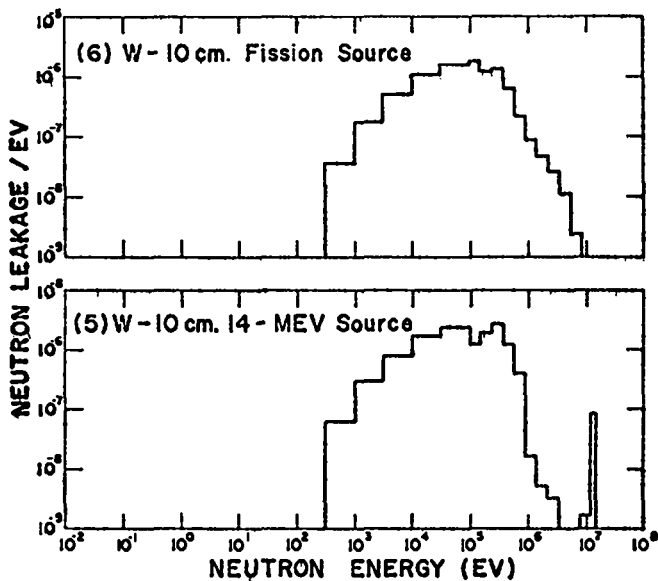


Fig. 8. Neutron leakage spectra from a tungsten "fast moderator" assembly. (Ordinate normalized to one source neutron.)

It will be noted in Table V that for several of the moderators the indicated total leakage is greater than 100%. This apparent "neutron multiplication" is due to the large  $(n, 2n)$  cross section in lead and tungsten.

#### Neutron Response of Simulated Scrap Barrels

An extensive program of neutron transport calculations has been undertaken in Group N-6 to guide experimental investigations of nondestructive scrap assay techniques. Present calculations using the one-dimensional DTF-IV transport code are concerned with simulated scrap barrels and the expected delayed neutron response from small amounts of fissile material interspersed in large amounts of scrap. The standard 55-gallon scrap barrel is simulated by a sphere of radius 30 cm--the radius of a standard 55-gallon drum.

The simulated barrel, or drum, is filled with moderating or matrix material plus a total of one gram of  $^{235}\text{U}$  distributed (in a spherical shell) at various radii. Representative moderating or matrix materials were chosen as follows: (1) hydrogenous material (polyethylene), (2) low-Z material (carbon), (3) medium-Z material (iron), and (4) high-Z material (lead). Four average material densities were assumed in the calculations: full density (quite unrealistic in the case of iron and lead, since this would load a 55-gallon drum to 3600 lbs. and 5200 lbs., respectively), and three representative densities which would load a 55-gallon drum to 50 lbs., 100 lbs., and 200 lbs. In actual practice, simple handling and safety considerations tend to keep the weight of individual scrap barrels to within a few hundred pounds at most. To simulate the practical case of a scrap barrel containing mostly paper trash, gloves, rags, Kim-wipes, etc., additional calculations were carried out for hydrogenous material at several very low densities. The fissile material (1 gm. of  $^{235}\text{U}$ ) was separately placed (distributed) at two radii in the barrel: at the center and at  $0.5R$  (15 cm). The

primary neutron source was distributed around the surface of the barrel (i. e., source evenly distributed in a surface shell due to the one-dimensional geometry of the DTF-IV code).

Two calculations were performed for each variation of moderator material, moderator density,  $^{235}\text{U}$  position, and neutron source energy. The first calculation gives the number of fissions occurring in the  $^{235}\text{U}$  and the energy at which they took place. From these fission yield data, together with delayed neutron absolute yields per fission and the energy spectrum of delayed neutrons, the number and energy distribution of delayed neutrons are computed. In the second calculation the primary neutron source is removed and the fission-produced delayed neutrons are taken as a distributed neutron source at the location(s) of the  $^{235}\text{U}$  in the barrel. With this delayed neutron source, the net neutron leakage out of the barrel is then computed as a function of energy. Such two-step delayed neutron response calculations have been carried out for four moderating materials at several densities with one gram of  $^{235}\text{U}$  at  $r = 15$  cm using both a 14-MeV neutron source and a  $1/E$  "tailored spectrum" source. Calculations have also been carried out for the 14-MeV source with the  $^{235}\text{U}$  at the center of the barrel. The results of all calculations to date are shown in Figs. 9, 10, and 11. (The two  $^{235}\text{U}$  positions, at  $r = 0$  and  $r = 15$  cm, are represented by dashed and solid curves, respectively.)

These neutron transport calculations point up the very useful general result that barrels containing almost any common scrap material other than hydrogenous material, and weighing up to a few hundred pounds, appear empty, or are essentially "transparent," to 14-MeV neutrons (Fig. 9). Even the hydrogenous materials, when present in low densities (e. g., in "light" scrap barrels containing paper trash, rags, filters, etc.), are essentially transparent to 14-MeV neutrons and should pose no serious problems as regards fast neutron interrogation and assay. It is clear, however,

from Figs. 9 and 10 that large amounts (i. e., high densities) of hydrogenous material (if not known to be present, and hence not taken into account) would give greatly enhanced delayed neutron response with a consequent overestimation of the amount of fissile material present in the scrap container. A measurement of the cadmium ratio (cf. Fig. 11)--the ratio of total neutron counts to those above  $\sim 0.3$  eV--may provide a very convenient indication of hydrogenous scrap present.

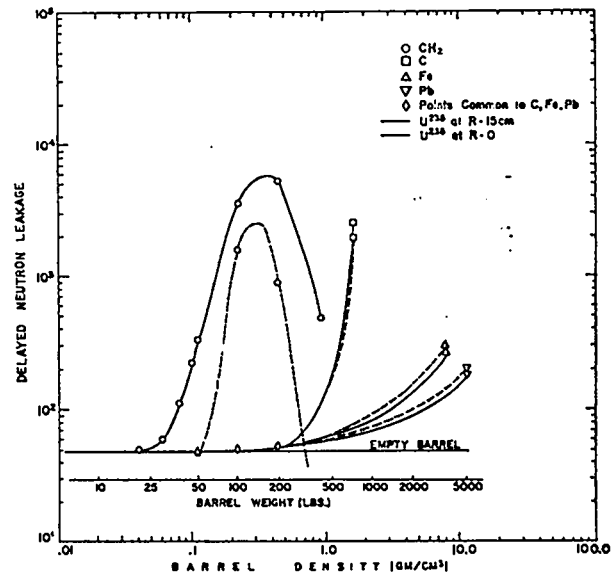


Fig. 9. Delayed neutron response of a simulated scrap barrel containing one gram of  $^{235}\text{U}$  in representative moderator or matrix materials--14-MeV source. (The base line labelled "empty barrel" refers to one gram of  $^{235}\text{U}$  in a barrel containing no other material.)

It is obvious from a comparison of Figs. 9 and 10 that the delayed neutron response using a  $1/E$  moderated-spectrum source differs quite drastically from the response using a 14-MeV source. Considerations of neutron penetrability and discrimination against threshold fissioning species (such as  $^{238}\text{U}$ ) suggest that the tungsten "fast moderated spectrum" source (cf. Fig. 8) may offer real advantages for neutron interrogation of scrap barrels as well as other containers. This possibility and other approaches to the complex problem



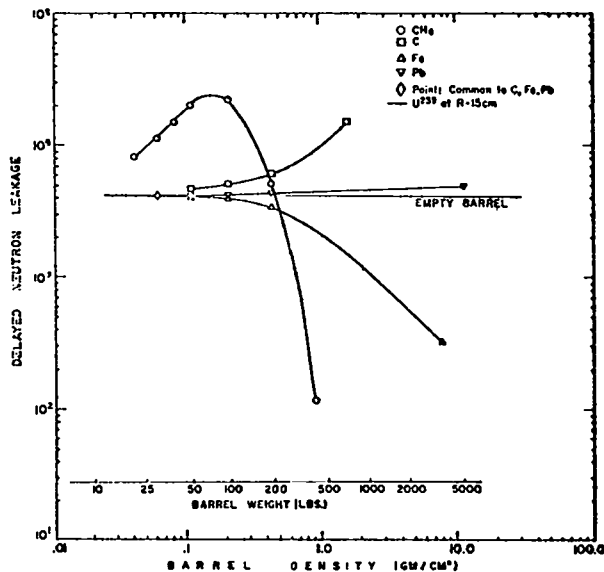


Fig. 10. Delayed neutron response of simulated scrap barrels containing one gram of  $^{235}\text{U}$  in representative moderator or matrix materials--1/E moderated source. (The base line labelled "empty barrel" refers to one gram of  $^{235}\text{U}$  in a barrel containing no other material.)

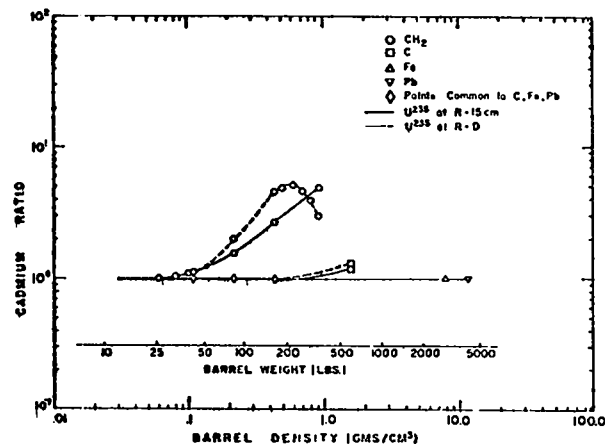


Fig. 11. Cadmium ratio for delayed neutron response of simulated scrap barrels.

of nondestructive scrap assay are being examined in both the experimental and computational portions of the LASL safeguards research program.

#### Modification of Neutron Transport Codes to Include Delayed Neutrons

The Los Alamos standard DTF neutron transport code has been modified, in the zero prompt lifetime approximation, to include full six-group delayed neutron time-dependent kinetic behavior,

With the modified code one can calculate directly the concentration of each delayed neutron precursor from each fission species present in a given system and the resulting time-dependent detector response.

The delayed neutron transport theory code is presently being used to study the effects of sample size and neutron multiplication upon the kinetic response method of nondestructive isotopic assay.

### AUXILIARY ASSAY TECHNIQUES USING FISSION DELAYED GAMMA RAYS

As previously noted (LA-3741), delayed fission gamma rays may either provide unique isotopic signatures or complement delayed neutron

assay methods already developed, depending on the specific gamma-ray characteristics measured and the detection and analysis techniques used. In par-

ticular, the measurement of gross delayed gamma-ray intensities over the time range from  $\sim 0.1$  sec to 100 sec after fission may offer a promising supplement to delayed neutron assay techniques.

Essentially all delayed gamma rays emitted 1 ms or more after fission result from de-excitation of nuclear states populated by  $\beta$  decay. Since nearly all primary fission fragments undergo  $\beta$  decay, the energy spectrum of delayed gamma rays is very complex and individual gamma-ray lines may be resolved only with very high-resolution detectors, such as Ge(Li). Presently available high-resolution gamma-ray data are insufficient for direct application to a practical assay system based on individual gamma-ray yield variations among

the major fission isotopes; on the other hand, basic data on gross fission product activity exist for the fission isotopes of major interest to nuclear safeguards (Phys. Rev. 134, B796-B823 (1964)).

The yield systematics of delayed gamma rays are quite similar to those for delayed neutron yields, i.e., longer average fission chain lengths correlate directly with larger fission yields. This similarity is illustrated in Fig. 12, which shows gross delayed neutron and gamma-ray activities versus time for neutron-induced fission of  $^{235}\text{U}$  and  $^{238}\text{U}$ . The systematics indicated in this figure is typical and applies generally to the major fission species.

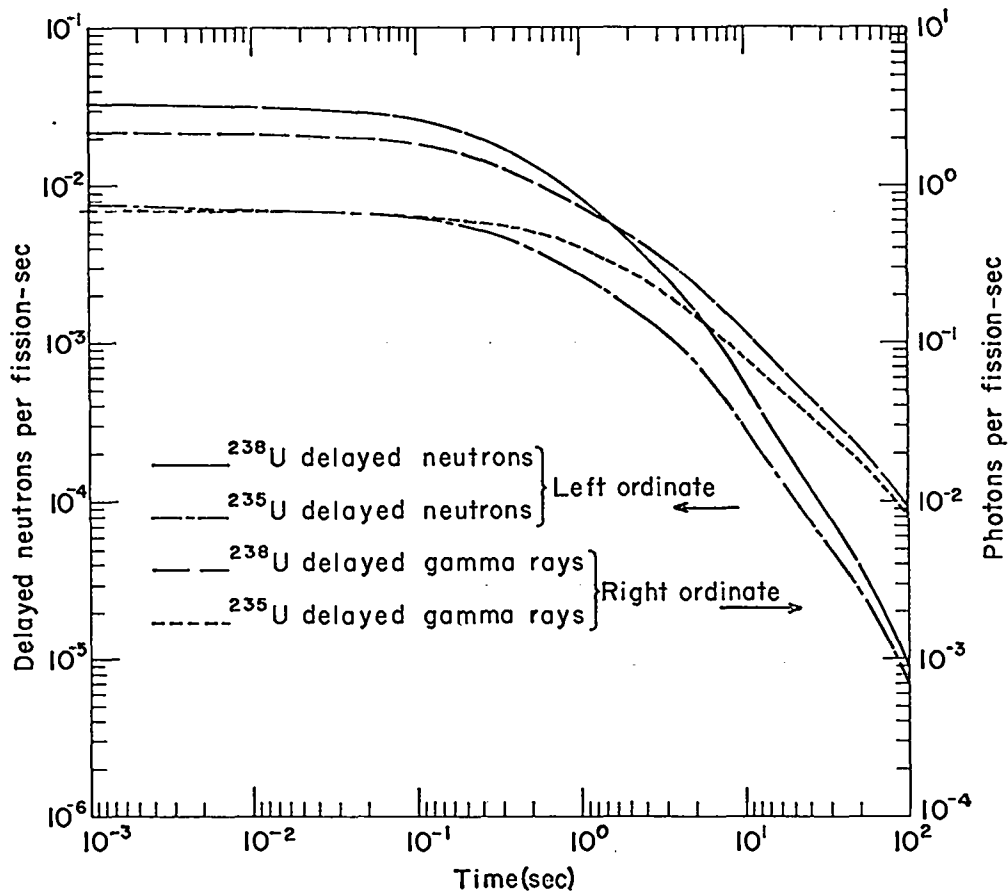


Fig. 12. Gross delayed neutron and gamma-ray activities versus time for neutron-induced fission of  $^{235}\text{U}$  and  $^{238}\text{U}$ .

An isotopic assay technique based on delayed gamma-ray decay characteristics can be formulated in the same way as the delayed neutron kinetics response method. The delayed gamma-ray activities from  $^{235}\text{U}$  and  $^{238}\text{U}$  have been fitted accurately with only five exponentials for times up to  $2 \times 10^3$  sec after fission. The resulting gross gamma-ray "periods and abundances" are given in Table VI.

The correlation between delayed neutron and gamma-ray yields for different fission isotopes is further illustrated in Fig. 13. Here, ratios of the gamma-ray abundances ( $b_j$ ) for  $^{238}\text{U}$  and  $^{235}\text{U}$  fission and corresponding ratios of delayed neutron abundances ( $a_i$ ) are plotted as a function of the appropriate group periods. It is apparent that isotopic analysis based on gross delayed gamma-ray decay is complementary to the delayed neutron kinetics method of assay.

Because of differences in neutron and gamma-ray penetrabilities in various materials, the simultaneous measurement of delayed gamma rays and neutrons may be useful for some assay applications in which the environment of the nuclear material is unknown, e.g., high-density scrap analysis.

For very short times after neutron-induced fission of  $^{235}\text{U}$  and  $^{239}\text{Pu}$ ,  $\sim 10^{-6}$  to  $5 \times 10^{-4}$  sec, 9 prominent gamma rays have been observed with

energies between 205 and 1330 keV. These gamma rays result from the decay of four fission fragment isomers with half-lives in the range of 3.4 - 80  $\mu\text{sec}$  and fission yields between 0.3 and 1.3%. The yields of individual isomeric gamma rays from  $^{235}\text{U}$  and  $^{239}\text{Pu}$  differ significantly and hence constitute a possible basis for isotopic assay; however, the corresponding data for other relevant nuclei, e.g.,  $^{238}\text{U}$ , are not available.

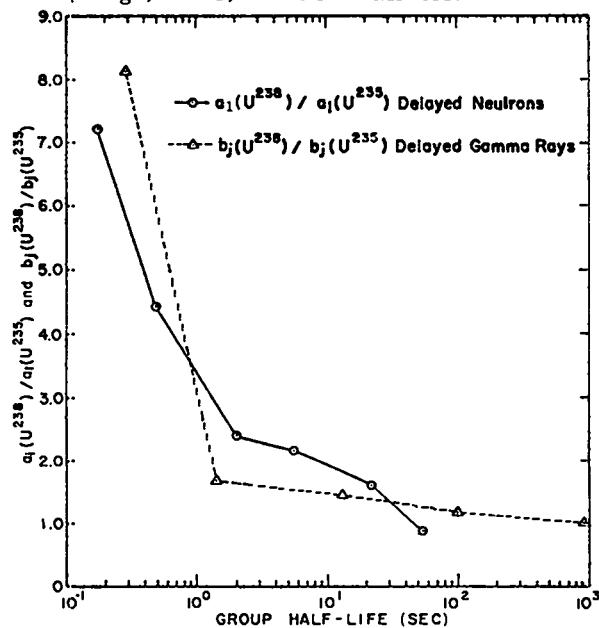


Fig. 13. Ratios of delayed neutron abundances  $a_i(^{238}\text{U})/a_i(^{235}\text{U})$  and delayed gamma-ray abundances  $b_j(^{238}\text{U})/b_j(^{235}\text{U})$  as functions of the appropriate group periods.

TABLE VI  
PERIODS AND ABUNDANCES FOR DELAYED GAMMA RAYS  
FROM NEUTRON-INDUCED FISSION OF  $^{235}\text{U}$  AND  $^{238}\text{U}$

Period (j)	$T_{1/2}^j$ (sec)	$\lambda_j$ (sec $^{-1}$ )	Abundances (Percent/Fission)	
			$b_j(^{235}\text{U})$	$b_j(^{238}\text{U})$
1	$2.9 \times 10^{-1}$	$2.4 \times 10^0$	$6.7 \times 10^0$	$5.4 \times 10^1$
2	$1.7 \times 10^0$	$4.1 \times 10^{-1}$	$1.05 \times 10^2$	$1.76 \times 10^2$
3	$1.3 \times 10^1$	$5.3 \times 10^{-2}$	$1.92 \times 10^2$	$2.81 \times 10^2$
4	$1.0 \times 10^2$	$6.9 \times 10^{-3}$	$1.73 \times 10^2$	$2.02 \times 10^2$
5	$9.4 \times 10^2$	$7.4 \times 10^{-4}$	$1.55 \times 10^2$	$1.55 \times 10^2$

## DETECTOR AND INSTRUMENTATION DEVELOPMENT

Two versatile, high-efficiency neutron detectors of the slab design developed in Group N-6 (cf. LA-3859-MS) have been constructed and are presently being used for applications requiring large area or large-solid-angle neutron detection. These detectors will also be used as coincidence counters to study the feasibility of detecting neutrons from  $^{240}\text{Pu}$  spontaneous fission in a background of  $(\alpha, n)$  neutrons.

The slab detector consists of thirteen, 6-atmosphere,  $^3\text{He}$  proportional counters (1" O. D. by 20" long) imbedded in two slabs of neutron moderator (polyethylene). These slabs are positioned in tandem inside a  $\text{B}_4\text{C}$  + Paraffin shield with an open face on one side for neutron entry. Additional neutron moderating and absorbing materials may be inserted in front of and between the slabs in order to vary the energy dependence of the detector.

Exterior features of the slab detector are illustrated in Figure 14. The detector presents a very large sensitive area (20" x 24"), having an intrinsic efficiency (for detecting neutrons incident on the sensitive area) of about 10%. The entire unit, including shield, weighs approximately 350 pounds; if desired, the unit can be disassembled into a number of relatively light-weight pieces within a few minutes.

Figure 15 shows a cross-sectional view of an N-6 slab detector which can be used to provide coarse neutron energy-spectrum information ("spectral indices"). When used in this "energy discrimination" mode, the front and back slabs are separated by 3 inches of polyethylene and are operated as two independent banks of counters. The cadmium sheets indicated in Fig. 15 prevent the diffusion of thermal neutrons into the detector banks. Since neutron attenuation in  $\text{CH}_2$  falls off rapidly with increasing neutron energy, the ratio of the response of the front counter bank to that of the back counter bank provides a sensitive measure of the

"average" energy of the incident neutrons.

An energy calibration of the front/back ratio of the slab detector operating in the "energy-discrimination" mode was performed using the following neutron sources: PuBe and  $^{252}\text{Cf}$  (continuous spectra with  $\bar{E}_n \approx 4.3$  and 2.2 MeV, respectively), and monoenergetic photoneutrons ( $E_n = 0.025, 0.26, \text{ and } 0.97$  MeV) from  $\text{Be}(\gamma, n)$  and  $\text{D}(\gamma, n)$  reactions initiated by gamma rays from the decay of  $^{124}\text{Sb}$  and  $^{24}\text{Na}$ . For these calibration measurements only 3 of the 6 counters in the front bank were connected. Results of these energy calibration measurements are presented in Fig. 16.

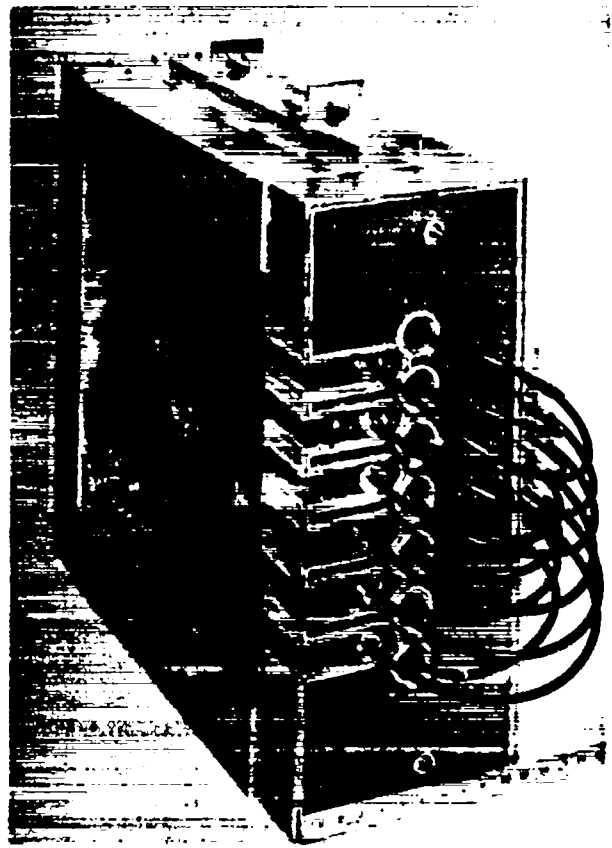


Fig. 14. General view of the N-6 slab neutron detector.

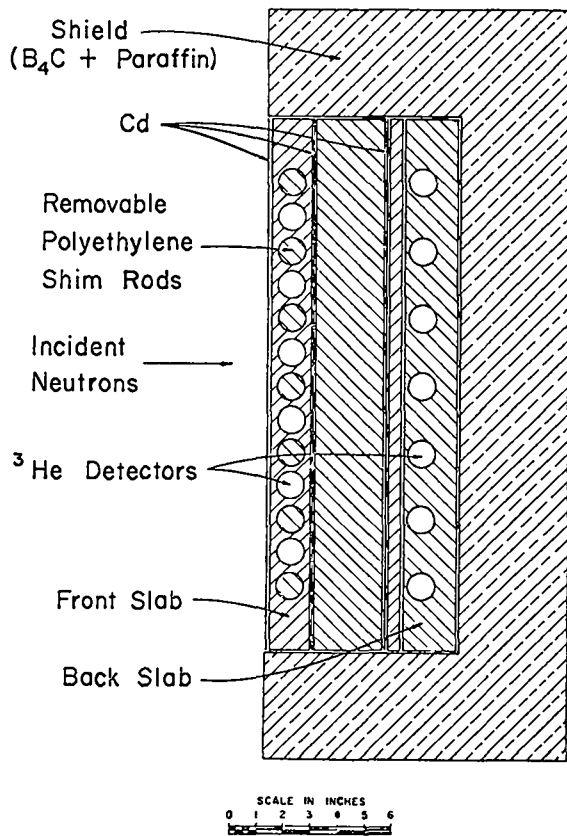


Fig. 15. Cross-sectional view of the N-6 slab detector. This configuration is used to obtain coarse neutron-energy spectrum information. In the "flat-response" mode of operation, all materials between the front and back counter banks are removed.

The front/back ratio for the configuration shown in Fig. 16 was also calculated as a function of incident neutron energy using the Los Alamos DTF-IV neutron transport code. The calculations were performed in slab geometry with a buckling term added to correct for the finite height and width of the detector. For the DTF-IV one-dimensional approximation, the  $^3\text{He}$  in the counters was assumed to be uniformly mixed with  $\text{CH}_2$  moderator and distributed over a region of thickness equal to the counter diameter (1 inch). Gas density was adjusted to preserve the total amount of  $^3\text{He}$  in the counters. The ratio of calculated  $^3\text{He}(n, p)$  reactions for each energy group in the front and back

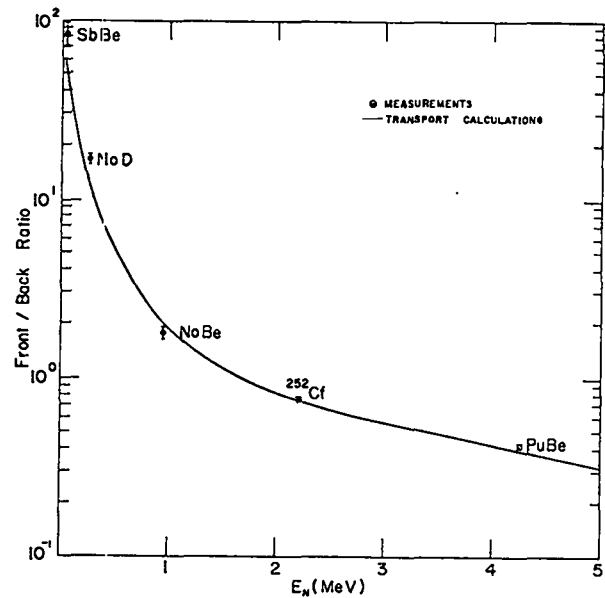


Fig. 16. Response ratios between front and back counter banks of the N-6 slab detector versus incident neutron energy. The points (with error bars) represent measured results, and the smooth curve shows the front/back ratio calculated using a one-dimensional transport code.

counter banks was used to obtain the overall (energy averaged) front/back ratio. Since the individual counters within each counter bank are separated by a thickness of  $\text{CH}_2$  about equal to the counter diameter, somewhat less than the actual amount of  $\text{CH}_2$  in the mock 1-inch thick layer is effective in the calculated neutron detection efficiency. This effect is particularly important for the front bank of counters, since neutron detection efficiency is most sensitive to moderator thickness for small thicknesses. Accordingly, the distributed density of the  $\text{CH}_2$  in the "front-counter" region was reduced until the calculated front/back ratio agreed with the experimental ratio at one energy (2 MeV).

Front/back ratios were then computed as a function of incident neutron energy using this reduced  $\text{CH}_2$  density, and the results are shown as the smooth curve in Fig. 16. The agreement between the calculations and measurements is quite satisfactory, particularly in view of the approximations inherent in the one-dimensional calculation.

When the slab detector is operated in the "flat-response" or "energy-independent" mode, the moderating and absorbing materials between the counter banks (as shown in Fig. 15) are removed, and the outputs of the two counter banks are connected in parallel. The removable polyethylene shim rods between the counters in the front slabs provide a means for flattening the overall detection efficiency as a function of incident neutron energy.

A pulse height distribution obtained with all 13 counters of a slab detector operating in parallel ("flat-response" mode) is shown in Fig. 17. The individual counters were matched to within 3% in output pulse height for thermal neutrons. All counter output channels were fed to a single special prototype FET preamplifier, developed in Group N-6. The overall pulse height resolution resulting

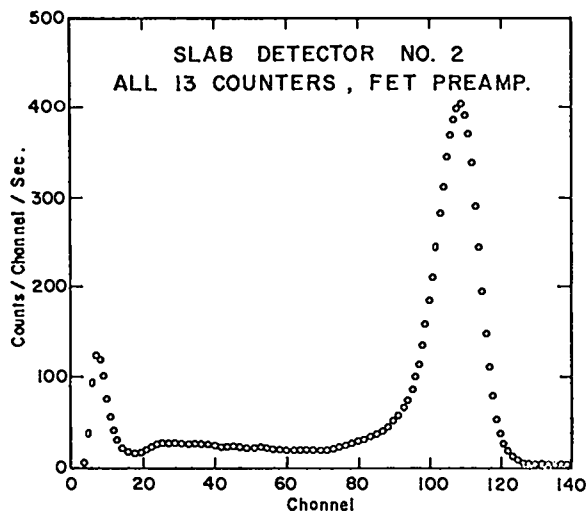


Fig. 17. Pulse height distribution of the N-6 slab detector. All 13 counters were operated in parallel using a single FET preamplifier.

from the 13 counters in combination is 12%, which is comparable to typical individual counter pulse height resolutions of 8-9%. The advantages of such good resolution of the output pulses from the FET preamplifier and multiple-counter combination are: (1) efficient rejection of pileup pulses from high gamma-radiation fields, and (2) high stability of overall counting systems.

The relatively low gamma-ray sensitivity of the N-6 slab detector (in 13-counter combination) is indicated by the fact that a 50 mr/hr gamma-ray field increases the ambient background counting rate by less than 10%.

#### 4 $\pi$ Neutron Detector

Fabrication of the high-efficiency  $4\pi$  neutron detector (described in LA-3802-MS) has been completed except for assembly of the shield and wiring of the high-voltage junction boxes. The high-pressure  $\text{BF}_3$  counters for this detector have been received and tested for closely-matched pulse height and resolution. As in the case of the N-6 slab detector, this close matching of individual counters will permit parallel operation of a large number of such counters without requiring individual operating voltage adjustments.

A photograph of the polyethylene moderating block for the  $4\pi$  detector is shown in Fig. 18. The very high overall efficiency of this detector (> 50%) will be especially advantageous for delayed-neutron assay applications requiring extremely high sensitivity (e. g., for small samples and/or low neutron source intensities).

#### Preamplifier Development

A general purpose charge sensitive preamplifier using field-effect transistors has been developed for use with proportional, solid state, and scintillation detectors. Some of the features of this preamplifier are:

- (1) Lower noise than preamplifiers presently in use.

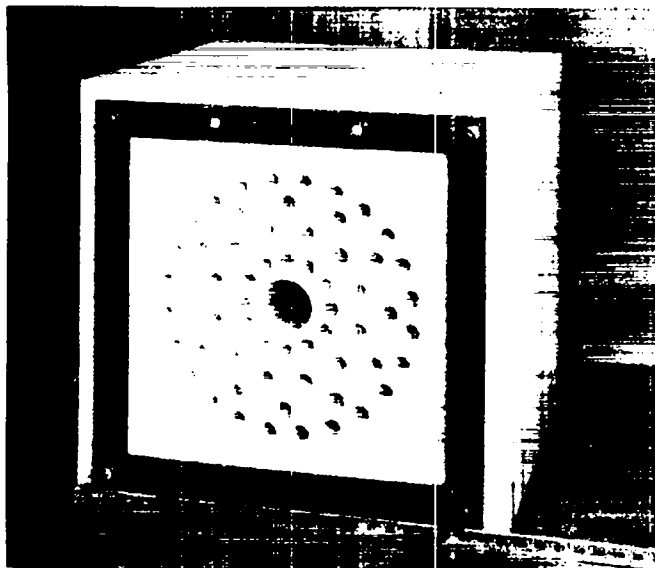


Fig. 18. Polyethylene moderating block for the high-efficiency  $4\pi$  neutron detector.

- (2) Low sensitivity to input capacity.
- (3) Both long (nominally 50  $\mu$ s decay) or short (nominally 2  $\mu$ s) output pulses available. Short output pulse pole-zero compensated.
- (4) Fast off-gating.
- (5) Output linear to 2 V into 100 ohm load.
- (6) Single + 12 V power supply required.
- (7) Charge sensitivity and output pulse shape (rise and fall times) may be

varied over large ranges by simple component changes in order to meet the varying requirements of different experiments and detectors.

- (8) Input protected against large voltage transients.

This FET preamplifier has proven to be particularly useful with the N-6 slab neutron detectors because of the high capacitance associated with parallel operation of all thirteen  $^3\text{He}$  counters.

#### ACCELERATORS AND NEUTRON SOURCES; USE AND DEVELOPMENT

Group N-6's new high-intensity mobile neutron source, "Accelerator I," was delivered to Los Alamos January 15, 1968, on an interim-loan basis by Picker Nuclear Corporation (marketing firm for Accelerators, Inc., the manufacturer). Accelerator I is a 150 kV, 3.5 ma compact positive ion accelerator; the unit met full dc current specifications within one week. In addition to pre- and post-deflection systems for microsecond beam pul-

sing, the accelerator is equipped for beam modulation by gating the RF (radiofrequency-discharge) ion source on and off. This new gating system provides extremely low background between pulses, but has required considerable "de-bugging." Also, to give better high-voltage stability in the pulsed mode of operation, an auxiliary bleeder resistor string was added to provide greater high-voltage bleeder current (1.5 ma, as compared to

300  $\mu$ a as delivered). The accelerator became completely operational the first of March 1968, and is currently undergoing stringent performance tests and evaluation for safeguards applications. Accelerator I is now performing extremely well with true beam-on/beam-off ratios of greater than  $10^9$  (disregarding activation and room-return neutron sources).

During this reporting period, the 350-kV

Cockcroft-Walton Accelerator continued to be used primarily for nuclear safeguards research and some weapons-related studies.

As part of Group N-6's continuing survey of commercially-available small, compact neutron sources, inspection visits have been made to Kaman Nuclear Corporation of Colorado Springs, Colorado, and to Sandia Corporation of Albuquerque, New Mexico.

### DENSE PLASMA FOCUS SOURCE

The N-6 Dense Plasma Focus (DPF) source, which was completed during the previous reporting period, is now undergoing an intensive program of testing, debugging, and modification, with the intended goal of increasing total neutron burst yield, reproducibility of yield, reliability, and ease of operation.

In the period from 1 January to 9 February, the DPF was fired 247 times. Of these, 81 shots gave measurable yields varying from  $5 \times 10^6$  to  $4.8 \times 10^9$  neutrons in bursts of 50-100 nanoseconds width. These shots were made using the strip-line dielectric switches described in earlier progress reports. With dielectric switching, the threshold voltage for neutron production was found to be 16 kilovolts, using at least eight of the twelve 15-mfd 20-kV capacitors available in the storage bank (i. e., 13.8 kilojoules of energy were dissipated). Yields in excess of  $10^9$  neutrons per burst required the full bank of 12 capacitors operating at 18.5 kilovolts with a total energy release of 26 kilojoules. Also with dielectric switching, a three-to-five minute interval was required between shots to prepare the DPF for re-firing. Extensive cleanup of greasy soot deposits liberated by burning of the mylar and silicone grease was required following each shot. Even so, residual soot accumulation eventually caused a major voltage arc-over in Feb-

ruary which seriously damaged many of the energy storage and switching components of the DPF source. For these reasons, and because the dielectric switches appeared to be firing in a non-reproducible manner, it was decided to convert to a switching system of vacuum spark gaps similar to that developed by Mather and Williams at LASL (Rev. Sci. Inst. 31, 279 (1960)). Accordingly, four vacuum spark gaps, each capable of handling the discharge from three capacitors, have been paralleled to switch current from the full twelve-capacitor bank through the DPF discharge gun. These spark gaps had been designed for coaxial-cable coupling to their load, but were adapted for our strip-line system in order both to minimize the amount of fabrication necessary for the conversion and to reduce system inductance and eliminate the problem of cable failures.

The new vacuum spark gap switches have now been installed, and neutron yields have already been obtained using only six capacitors charged to as little as 10 kilovolts, with a total energy release of 4.1 kilojoules. This is to be contrasted with a minimum energy-release requirement of 13.8 kilojoules under the old dielectric switching method of operation. Using six capacitors, neutron yields in excess of  $10^9$  have been consistently obtained, and a maximum yield of  $3.5 \times 10^9$  neutrons has already



been produced by an 18-kilovolt discharge from 6 capacitors (13 kilojoules). Based on these results, it appears that with dielectric switches at least half of the total electrical energy was being dissipated in the switching system itself, rather than being delivered to the gas plasma.

Some difficulties with cracking of the glass insulators in the dielectric switches have arisen. Certain minor design changes in switch geometry, annealing the glass after fabrication, or complete replacement of glass with ceramic insulators are

being explored as possible solutions to this problem.

An important advantage which has accrued from the replacement of dielectric switches with vacuum spark gaps has been a sharp increase in the rate at which the DPF source can be repetitively fired. More than one burst per minute is now easily attained, thus permitting significant acceleration of the testing and evaluation program on the DPF source for nuclear safeguards applications.

## OTHER CONTRIBUTIONS TO NUCLEAR SAFEGUARDS RESEARCH AT LASL

### Foil Preparation (CMF-4, CMB-6)

Several deposits of  $^{239}\text{Pu}$ ,  $^{235}\text{U}$ ,  $^{233}\text{U}$ , and  $^{232}\text{Th}$  were evaporated on platinum backing discs for use in fission chambers. In addition, two foils each of  $^{10}\text{B}_2\text{O}_3$  and  $^6\text{LiF}$  were supplied.

### Plutonium Foil Analysis (N-2)

The precise mass of three plutonium foils was determined by absolute  $\alpha$ -counting in Group N-2's calibrated low-geometry alpha chamber.

### Plutonium Sample Preparation (CMB-11)

Three 2"-diameter disc samples of plutonium (0.010", 0.020", and 0.050" thickness) have been prepared and sealed in 0.010"-wall copper cans.

### $^{238}\text{Pu}$ -Li Source Fabrication and Inspection

(GMX-1, W-1, CMB, CMF)

Several LASL groups are contributing to the preparation of a new  $^{238}\text{Pu}$ -Li source, free of fluorine and exhibiting special energy-spectrum characteristics:

GMX-1: Radiographic inspection of the new source container. Also,

radiographic inspection of the old  $^{238}\text{Pu}$ -Li source to verify the integrity of the containment.

W-1: Pressure testing of dummy source containers to determine failure point.

CMB-11: Major responsibility for preparation of the new fluorine-free  $^{238}\text{Pu}$ -Li source.  $^{238}\text{Pu}$  in nitride form will be chemically prepared and mixed in a special fluorine-free ball mill with  $^7\text{Li}_2^{16}\text{O}$  furnished by CMF-4.

### Tritium Target Preparation for N-6 Cockcroft-Walton Accelerator (CMF-4)

### Development of Group-Averaged Cross Sections (T-7)

Group-averaged cross sections for twelve nuclides of interest have been calculated from the data in the LASL Evaluated Nuclear Data Library. These 25-group cross section sets, in punched-card decks, are now being used in the DTF-IV neutron transport calculations described in this report.